Online Precoding Design for Downlink MIMO Wireless Network Virtualization with Imperfect CSI

Juncheng Wang*, Min Dong†, Ben Liang*, and Gary Boudreau‡
*Department of Electrical and Computer Engineering, University of Toronto, Canada, ‡Ericsson Canada, Canada
†Department of Electrical, Computer and Software Engineering, University of Ontario Institute of Technology, Canada

***Abstract*—We consider online downlink precoding design for multiple-input multiple-output (MIMO) wireless network virtualization (WNV) in a fading environment with imperfect channel state information (CSI). In our WNV framework, a base station owned by an infrastructure provider (InP) is shared by several service providers (SPs) that are oblivious to each other. The SPs design their virtual MIMO transmission demands to serve their own users, while the InP designs the actual downlink precoding to meet the service demands from the SPs. Therefore, the impact of imperfect CSI is two-fold, on both the InP and the SPs. We aim to minimize the long-term time-averaged expected precoding deviation, considering both long-term and short-term transmit power limits. We propose a new online MIMO WNV algorithm to provide a semi-closed-form precoding solution based only on the current imperfect CSI. We derive a performance bound for our proposed algorithm and show that it is within an $O(\delta)$ gap from the optimum over any given time horizon, where δ is a normalized measure of CSI inaccuracy. Simulation results with two popular precoding techniques validate the performance of our proposed algorithm under typical urban micro-cell Long-Term Evolution network settings.**

I. Introduction

Wireless network virtualization (WNV) aims at sharing common network infrastructure among multiple virtual networks to reduce the capital and operational expenses of wireless networks [1]. In WNV, the infrastructure provider (InP) virtualizes the physical wireless infrastructure and radio resources into virtual slices; the service providers (SPs) lease these virtual slices and serve their subscribing users under their own management and requirements [2]. Different from wired network virtualization, WNV concerns the sharing of both the wireless hardware and the radio spectrum. The random nature of the wireless medium brings new challenges in guaranteeing the isolation of virtual networks [3].

In this work, we focus on downlink WNV in a multiple-input multiple-output (MIMO) system where one InP-owned base station (BS) with multiple antennas is shared by multiple SPs to serve their subscribing users. Most prior MIMO WNV studies consider strict physical isolation, where the InP allocates exclusive subsets of antennas or orthogonal sub-channels to each SP [4]-[9]. This approach of physical isolation is inherited from wired network virtualization [10]. It does not fully utilize the benefit of spatial spectrum sharing enabled by MIMO beamforming. In contrast, in [11], the SPs are allowed to share all antennas and spectrum resources simultaneously. The SPs design their own virtual precoding matrices as virtualization demands, based on their own users' local channel states and service demands. Since the SPs are oblivious of each other, straightforward implementation of their demanded precoding matrices would induce an unacceptable amount of interference among them. Thus, the InP must intelligently design the actual downlink precoding to mitigate the inter-SP interference, while satisfying the SPs' virtualization demands. It has been demonstrated in [11] that, with an optimally designed InP precoding matrix, such a spatial isolation approach substantially outperforms the physical isolation approach. In this work, we adopt the same virtualization method as in [11].

All of the above works on MIMO WNV have focused on per-slot design optimization problems subject to a per-slot transmit power constraint. Recognizing that the long-term average transmit power is an important indicator of energy usage [12], in this work, we further consider the optimal *online* design of MIMO WNV with an additional constraint on the long-term average transmit power. Our objective is to design optimal global downlink precoding at the InP to serve all users simultaneously, given the set of virtualization demands made locally by each SP to serve its own users. The optimization criterion is the long-term time-averaged expected deviation between the received signals from the actual precoding and those demanded by the SPs, with implicit elimination of interference among the SPs.

In practical wireless systems, there are unavoidable channel state information (CSI) errors induced by channel estimation, quantization, and imperfect feedback. This challenge is especially acute with MIMO fading channels, where the channel state space is large and the channel state can fluctuate quickly over time. Some existing MIMO WNV solutions can accommodate imperfect CSI [5], [7], [8], [11], but they only consider its impact on the InP. In contrast, in our problem, imperfect CSI has a two-fold impact, on both the InP and the SPs, since both of them rely on the channel state to design the actual and virtual precoding matrices.

The main contributions of this paper are summarized below:

- We formulate the above downlink MIMO WNV as an online precoding problem to share all antennas and wireless spectrum resources among the SPs for efficient resource allocation, accommodating both long-term and short-term transmit power constraints. In each time slot, each SP is allowed to locally demand its own precoder based on the imperfect local CSI without the need to be aware of the

This work has been funded in part by Ericsson Canada and by the Natural Sciences and Engineering Research Council (NSERC) of Canada.

other SPs. The InP designs the global precoder based on the imperfect global CSI to minimize the deviation between the SPs' demands and the actual received signals at their users. This implies implicit elimination of the inter-SP interference.

- We propose an online MIMO WNV algorithm, by extending the standard Lyapunov optimization to deal with imperfect CSI. Our proposed algorithm determines downlink precoding only based on the current imperfect CSI, and the online precoding solution is in semi-closed form. Our analysis shows that the performance of our proposed algorithm achieved with only the current imperfect CSI can be arbitrarily close to an $O(\delta)$ performance gap to the optimum achieved with perfect CSI over any given time horizon, where δ is a normalized measure of CSI inaccuracy. To the best of our knowledge, this two-fold impact of imperfect CSI on both the InP and the SPs has not been studied in the literature of WNV.
- Our simulation results, under typical urban micro-cell Long-Term Evolution (LTE) network settings, demonstrate that the proposed algorithm has fast convergence and is robust to imperfect CSI. We further demonstrate the performance advantage of the virtualized network enabled by the proposed algorithm over a non-virtualized network.

The rest of the paper is organized as follows. In Section II, we present the related work. Section III describes the system model and problem formulation. In Section IV, we present our online algorithm and precoding solution. Performance bounds are provided in Section V. Simulation results are presented in Section VI, followed by concluding remarks in Section VII.

II. Related Work

Among existing works of MIMO WNV that enforce strict physical isolation, [4] and [5] study the problems of throughput maximization and energy minimization, respectively. Both of them use the orthogonal frequency division multiplexing massive MIMO setting. A two-level hierarchical auction architecture is proposed in [6] to allocate exclusive sub-carriers among the SPs. The uplink resource allocation problems are investigated in [7] and [8], combining MIMO WNV with the cloud radio networks and non-orthogonal multiple access techniques, respectively. Antennas are allocated among the SPs through pricing for virtualized massive MIMO systems in [9]. In this work, we adopt the spatial isolation approach of [11], where virtualization is achieved by MIMO precoding design. It has been demonstrated in [11] that this approach substantially outperforms the strict physical isolation approach.

The general Lyapunov optimization technique [13] and online convex optimization technique [14] have been applied to solve various online problems in non-virtualized MIMO systems. For example, online projected gradient descent and matrix exponential learning are used in [15] and [16] for MIMO uplink covariance matrix design. Online power control for wireless transmission with energy harvesting and storage has been studied for single-hop transmission [17] and two-hop relaying [18]. Online downlink MIMO WNV with accurate CSI is studied in [19]. Dynamic transmit covariance design for point-to-point MIMO systems is studied in [20], by extending standard Lyapunov optimization to deal with inaccurate system state. Our online algorithm is inspired by [20], but our MIMO WNV problem is challenging with several key differences: 1) this is a virtualization demand and response mechanism between the InP and the SPs; 2) the SPs are oblivious to each other and share all antennas and wireless spectrum resources provided by the InP; 3) both the InP and the SPs design the actual and virtual precoding matrices based on imperfect CSI. These unique features of MIMO WNV bring new challenges to the algorithm design and the performance analysis that cannot be addressed by [20]. In particular, imperfect CSI has a two-fold impact on both the InP and the SPs, which requires new techniques to bound the virtualization performance in terms of the difference between the SPs' virtualization demand and the InP's actual precoding outcome.

III. System Model and Problem Formulation

A. System Model

We consider a virtualized MIMO cellular network formed by one InP and M SPs. In each cell, the InP owns the BS and performs virtualization at the BS for data transmission. The SPs are oblivious to each other and serve their own subscribing users. Other functional structures of the network, including the core network and computational resources, are assumed to be already virtualized.

Consider downlink transmissions in a virtualized cell, where the InP-owned BS is equipped with N antennas. The M SPs share the N antennas at the BS and the spectrum resources provided by the InP. Each SP m has K_m users, for a total of $K = \sum_{m\in\mathcal{M}} K_m$ users in the cell. Let $\mathcal{N} = \{1, \ldots, N\}$, $\mathcal{M} = \{1, \ldots, M\}$, $\mathcal{K}_m = \{1, \ldots, K_m\}$, and $\mathcal{K} = \{1, \ldots, K\}$.

We consider a time-slotted system with time indexed by t. Let $\mathbf{H}(t) \in \mathbb{C}^{K\times N}$ denote the MIMO channel state between the BS and all K users at time t. We assume a block fading channel model, where $\{\mathbf{H}(t)\}$ over time t is independent and identically distributed (i.i.d.). The distribution of $\mathbf{H}(t)$ is unknown and can be arbitrary. We assume that the channel gain is bounded by a constant $B \geq 0$ at any time t, given by

$$\|\mathbf{H}(t)\|_F \leq B, \quad \forall t \tag{1}$$

where $\|\cdot\|_F$ denotes the Frobenius norm.

We adopt the spatial virtualization approach first proposed in [11], which is illustrated in Fig. 1. Let $\mathbf{H}_m(t) \in \mathbb{C}^{K_m\times N}$ denote the channel state between the BS and K_m users of SP m. In the idealized case where the CSI is perfect, at each time t, the InP shares the channel state $\mathbf{H}_m(t)$ with SP m and allocates a transmission power P_m to the SP. Using $\mathbf{H}_m(t)$, each SP m designs its own precoding matrix $\mathbf{W}_m(t) \in \mathbb{C}^{N\times K_m}$, subject to the transmission power limit $\|\mathbf{W}_m(t)\|_F^2 \leq P_m$. The design of $\mathbf{W}_m(t)$ is solely based on the service needs of SP m's own users without considering the existence of the other SPs sharing the same antennas and spectrum resources. Each SP m then sends $\mathbf{W}_m(t)$ to the

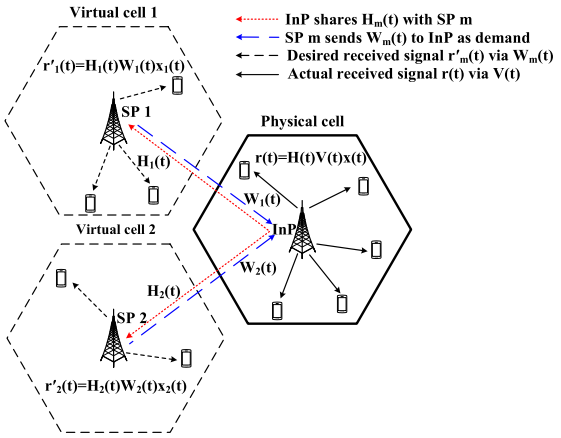

Fig. 1. An illustration of MIMO virtualization in a cell with one InP and two SPs each serving its own users in a virtual cell.

InP as a virtual precoding matrix by the SP. For SP m, with $\mathbf{W}_m(t)$, the virtual received signal vector $\mathbf{y}'_m$ (at its K_m users) is given by $\mathbf{y}'_m(t) = \mathbf{r}'_m(t) + \mathbf{n}_m(t)$, where $\mathbf{n}_m(t)$ is the received additive noise vector, and

$$\mathbf{r}'_m(t) = \mathbf{H}_m(t)\mathbf{W}_m(t)\mathbf{x}_m(t)$$

is the *desired* received signal vector (noiseless), with $\mathbf{x}_m(t)$ being the transmitted signal vector. Define $\mathbf{y}'(t) \triangleq [\mathbf{y}'^H_1(t), \ldots, \mathbf{y}'^H_M(t)]^H$ as the virtual received signal vector at all K users, we have $\mathbf{y}'(t) = \mathbf{r}'(t) + \mathbf{n}(t)$ where $\mathbf{r}'(t) = \mathbf{D}(t)\mathbf{x}(t)$ is the desired received signal vector, with $\mathbf{D}(t) \triangleq \text{blkdiag}\{\mathbf{H}_1(t)\mathbf{W}_1(t), \ldots, \mathbf{H}_M(t)\mathbf{W}_M(t)\} \in \mathbb{C}^{K\times K}$ being the virtualization demand made by all SPs, $\mathbf{x}(t) \triangleq [\mathbf{x}^H_1(t), \ldots, \mathbf{x}^H_M(t)]^H$, and $\mathbf{n}(t) \triangleq [\mathbf{n}^H_1(t), \ldots, \mathbf{n}^H_M(t)]^H$. The transmitted signals to all K users are assumed independent to each other, with zero-mean and unit power, *i.e.,* $\mathbb{E}\{\mathbf{x}(t)\} = \mathbf{0}$ and $\mathbb{E}\{\mathbf{x}(t)\mathbf{x}^H(t)\} = \mathbf{I}, \forall t$.

At each time t, the InP designs the actual downlink precoding matrix $\mathbf{V}(t) \triangleq [\mathbf{V}_1(t), \ldots, \mathbf{V}_M(t)] \in \mathbb{C}^{N\times K}$, where $\mathbf{V}_m(t) \in \mathbb{C}^{N\times K_m}$ is the actual downlink precoding matrix for SP m. The actual received signal vector $\mathbf{y}_m(t)$ at K_m users of SP m is given by $\mathbf{y}_m(t) = \mathbf{r}_m(t) + \mathbf{n}_m(t)$, where $\mathbf{r}_m(t)$ is the *actual* received signal vector (noiseless), given by

$$\mathbf{r}_m(t) = \mathbf{H}_m(t)\mathbf{V}_m(t)\mathbf{x}_m(t) + \sum_{i\in\mathcal{M}, i\neq m} \mathbf{H}_m\mathbf{V}_i(t)\mathbf{x}_i(t).$$

The second term in the last equation is the inter-SP interference from the other SPs to the users of SP m. The actual received signal vector $\mathbf{y}(t) \triangleq [\mathbf{y}^H_1(t), \ldots, \mathbf{y}^H_M(t)]^H$ at all K users is given by $\mathbf{y}(t) = \mathbf{r}(t) + \mathbf{n}(t)$ where $\mathbf{r}(t) = \mathbf{H}(t)\mathbf{V}(t)\mathbf{x}(t)$.

B. Problem Formulation

For downlink MIMO WNV, the InP designs precoding matrix $\mathbf{V}(t)$ to perform MIMO virtualization. Note that while each SP m designs its own virtual precoding matrix $\mathbf{W}_m(t)$ without considering the inter-SP interference, the InP designs the actual downlink precoding matrix $\mathbf{V}(t)$ to mitigate the inter-SP interference, in order to meet the virtualization demand $\mathbf{D}(t)$ received from the SPs.

With the InP's actual precoding matrix $\mathbf{V}(t)$ and each SP m's virtual precoding matrix $\mathbf{W}_m(t)$, the expected deviation of the actual received signal vector at all K users from the desired one is given by

$$\mathbb{E}\{\|\mathbf{r}(t) - \mathbf{r}'(t)\|_2^2\} = \mathbb{E}\{\|\mathbf{H}(t)\mathbf{V}(t) - \mathbf{D}(t)\|_F^2\}.$$

The goal at the InP is to optimize MIMO precoding to minimize the long-term time-averaged expected precoding deviation from the virtualization demand, subject to both long-term and short-term transmit power constraints. The optimization problem is formulated as follows:

$$\mathbf{P1}: \quad \min_{\{\mathbf{V}(t)\}} \quad \lim_{T\to\infty} \frac{1}{T}\sum_{t=0}^{T-1} \mathbb{E}\{\|\mathbf{H}(t)\mathbf{V}(t) - \mathbf{D}(t)\|_F^2\}$$

$$\text{s.t.} \quad \lim_{T\to\infty} \frac{1}{T}\sum_{t=0}^{T-1} \mathbb{E}\{\|\mathbf{V}(t)\|_F^2\} \leq \bar{P}, \tag{2}$$

$$\|\mathbf{V}(t)\|_F^2 \leq P_{\max} \tag{3}$$

where $\bar{P}$ is the average transmit power limit, and $P_{\max}$ is the maximum transmit power limit at the BS. Both power limits are set by the InP, and we assume $\bar{P} \leq P_{\max}$ to avoid triviality.

Since channel state $\mathbf{H}(t)$ is random, **P1** is a stochastic optimization problem. It is challenging to solve, especially when the distribution of $\mathbf{H}(t)$ is unknown due to the difficulty of measuring it in MIMO systems with a large number of antennas and users[1]. In addition, the instantaneous channel state cannot be obtained accurately in practical systems. Typically, the InP only has an inaccurate estimate of the channel state $\hat{\mathbf{H}}(t)$ at each time t. With given channel estimation quality, we assume that the normalized CSI inaccuracy is bounded by a constant $\delta \geq 0$ at any time t, given by

$$\frac{\|\tilde{\mathbf{H}}_m(t)\|_F}{\|\mathbf{H}_m(t)\|_F} \leq \delta, \quad \forall m \in \mathcal{M}, \quad \forall t \tag{4}$$

where $\tilde{\mathbf{H}}_m(t) \triangleq \mathbf{H}_m(t) - \hat{\mathbf{H}}_m(t)$ is the channel estimation error and $\hat{\mathbf{H}}_m(t)$ is the estimated channel state of SP m's users. It follows that at each time t, the estimated channel gain is bounded by

$$\|\hat{\mathbf{H}}(t)\|_F \leq \|\mathbf{H}(t)\|_F + \|\tilde{\mathbf{H}}(t)\|_F \leq B(1+\delta), \quad \forall t. \tag{5}$$

Thus, at each time t, each SP m only has the estimated channel state $\hat{\mathbf{H}}_m(t)$ shared by the InP to design its own virtual precoding matrix, denoted by $\hat{\mathbf{W}}_m(t)$. As a result, the InP receives an inaccurate virtualization demand from the SPs, defined as $\hat{\mathbf{D}}(t) \triangleq \text{blkdiag}\{\hat{\mathbf{H}}_1(t)\hat{\mathbf{W}}_1(t), \ldots, \hat{\mathbf{H}}_M(t)\hat{\mathbf{W}}_M(t)\}$. Based on $\hat{\mathbf{H}}(t)$ and $\hat{\mathbf{D}}(t)$, the InP then designs the actual precoding matrix, denoted by $\hat{\mathbf{V}}(t)$.

In this work, with unknown channel distribution and an inaccurate estimation of the instantaneous channel state at each time t, we aim to develop an online MIMO WNV algorithm based on $\hat{\mathbf{H}}(t)$ and $\hat{\mathbf{D}}(t)$ for a precoding solution $\{\hat{\mathbf{V}}(t)\}$ to **P1**.

[1]If the channel distribution is known, it is possible to solve **P1** through Dynamic Programming (DP) [21]. However, the DP method faces the curse of dimensionality in computational complexity and is impractical for real systems especially for large N and K.

IV. Online MIMO WNV Algorithm

In this section, we present a new online MIMO WNV algorithm that utilizes the Lyapunov optimization technique. Different from standard Lyapunov optimization that relies on accurate system state [13], we develop new techniques to design our online algorithm to accommodate imperfect CSI at both the InP and the SPs.

A. Online Optimization Formulation

To design an online algorithm for solving **P1**, we introduce a virtual queue $Z(t)$ for the long-term average transmit power constraint (2) with the updating rule given by

$$Z(t+1) = \max\{Z(t) + \|\hat{\mathbf{V}}(t)\|_F^2 - \bar{P}, 0\}. \tag{6}$$

Define $L(t) \triangleq \frac{1}{2}Z^2(t)$ as the quadratic Lyapunov function and $\Delta(t) \triangleq L(t+1) - L(t)$ as the corresponding Lyapunov drift at time t. Solving **P1** can be converted to minimizing the objective function while stabilizing the virtual queue through minimizing a drift-plus-penalty (DPP) metric [13], defined as $\mathbb{E}\{\Delta(t)|Z(t)\} + U\mathbb{E}\{\hat{\rho}(t)|Z(t)\}$, where $\hat{\rho}(t) \triangleq \|\hat{\mathbf{H}}(t)\hat{\mathbf{V}}(t) - \hat{\mathbf{D}}(t)\|_F^2$ and $U > 0$ is the relative weight. The DPP metric is a weighted sum of the conditional expectation on the Lyapunov drift $\Delta(t)$ and the penalty $\hat{\rho}(t)$ on precoding deviation under the current inaccurate channel state $\hat{\mathbf{H}}(t)$, given the current virtual queue length $Z(t)$. We first provide an upper bound for the DPP metric in the following lemma. The proof follows standard Lyapunov optimization techniques [13] and is omitted.

Lemma 1. At each time t, for any precoding design of $\hat{\mathbf{V}}(t)$, the DPP metric has the following upper bound for all $Z(t)$ and $U > 0$

$$\begin{aligned}&\mathbb{E}\{\Delta(t)|Z(t)\} + U\mathbb{E}\{\hat{\rho}(t)|Z(t)\}\\ &\le S + U\mathbb{E}\left\{\hat{\rho}(t)|Z(t)\right\} + Z(t)\mathbb{E}\{\|\hat{\mathbf{V}}(t)\|_F^2 - \bar{P}|Z(t)\}\end{aligned} \tag{7}$$

where $S \triangleq \frac{1}{2}\max\left\{(P_{\max} - \bar{P})^2, \bar{P}^2\right\}$.

Minimizing the DPP metric directly is still difficult due to the dynamics involved in the Lyapunov drift $\Delta(t)$. Instead, we minimize its upper bound given in Lemma 1, which is no longer a function of $\Delta(t)$. Specifically, given $\hat{\mathbf{H}}(t)$ at each time t, we consider the per-slot version of the upper bound in (7) by removing the conditional expectation and the constant terms as objective. The resulting per-slot problem is given as follows:

$$\begin{aligned}\mathbf{P2}: \quad \min_{\hat{\mathbf{V}}(t)} \quad & U\|\hat{\mathbf{H}}(t)\hat{\mathbf{V}}(t) - \hat{\mathbf{D}}(t)\|_F^2 + Z(t)\|\hat{\mathbf{V}}(t)\|_F^2\\ \text{s.t.} \quad & \|\hat{\mathbf{V}}(t)\|_F^2 \le P_{\max}.\end{aligned} \tag{8}$$

Note that **P2** is a per-slot precoding optimization problem under the current inaccurate channel state $\hat{\mathbf{H}}(t)$ and the virtual queue length $Z(t)$, subject to the short-term transmit power constraint (8) only. Compared with the original **P1**, the long-term time-averaged expected objective is modified to the per-slot version of DPP metric in **P2**, where the long-term average transmit power constraint (2) is converted to the queue stability in $Z(t)$ as part of the DPP metric. We solve **P2** to obtain the optimal precoding matrix $\hat{\mathbf{V}}^\star(t)$ for **P2** at each time t, and then update the virtual queue $Z(t)$ according to its queue dynamics in (6). An outline of the proposed online algorithm is given in Algorithm 1.

Algorithm 1 Outline of Online MIMO WNV Algorithm

1: Let $U > 0$ be a constant parameter and $Z(0) = 0$. At each time t, observe $\hat{\mathbf{H}}(t)$ and $Z(t)$, and then do the following:
2: Solve the per-slot problem **P2** for $\hat{\mathbf{V}}^\star(t)$ (see Section IV-B).
3: Update $Z(t+1) = \max\{Z(t) + \|\hat{\mathbf{V}}^\star(t)\|_F^2 - \bar{P}, 0\}$.

B. Online Precoding Solution to *P2*

Now we present a semi-closed-form solution to **P2**. We omit the time index t in solving **P2** for notation simplicity. Note that **P2** is essentially a constrained regularized least square problem. Since **P2** is a convex optimization problem satisfying the Slater's condition, the strong duality holds. We solve **P2** using the Karush-Kuhn-Tucker (KKT) conditions [22]. The Lagrange function for **P2** is given by

$$\begin{aligned}&L(\hat{\mathbf{V}}, \lambda) = U\|\hat{\mathbf{H}}\hat{\mathbf{V}} - \hat{\mathbf{D}}\|_F^2 + Z\|\hat{\mathbf{V}}\|_F^2 + \lambda(\|\hat{\mathbf{V}}\|_F^2 - P_{\max})\\ &= U(\mathrm{tr}\{\hat{\mathbf{H}}^H\hat{\mathbf{H}}\hat{\mathbf{V}}\hat{\mathbf{V}}^H\} + \mathrm{tr}\{\hat{\mathbf{D}}\hat{\mathbf{D}}^H\} - \mathrm{tr}\{\hat{\mathbf{H}}^H\hat{\mathbf{D}}\hat{\mathbf{V}}^H\}\\ &\quad - \mathrm{tr}\{\hat{\mathbf{H}}\hat{\mathbf{V}}\hat{\mathbf{D}}^H\}) + (Z+\lambda)\,\mathrm{tr}\{\hat{\mathbf{V}}\hat{\mathbf{V}}^H\} - \lambda P_{\max}\end{aligned}$$

where λ is the Lagrangian multiplier associated with constraint (8). The partial derivative of $L(\hat{\mathbf{V}}, \lambda)$ to $\hat{\mathbf{V}}^*$ is given by

$$\nabla_{\hat{\mathbf{V}}^*} L(\hat{\mathbf{V}}, \lambda) = U(\hat{\mathbf{H}}^H\hat{\mathbf{H}}\hat{\mathbf{V}} - \hat{\mathbf{H}}^H\hat{\mathbf{D}}) + (Z+\lambda)\hat{\mathbf{V}}. \tag{9}$$

where the partial derivative expression follows from $\nabla_{\mathbf{B}^*}\mathrm{tr}\{\mathbf{A}\mathbf{B}^H\} = \mathbf{A}$ and $\nabla_{\mathbf{B}^*}\mathrm{tr}\{\mathbf{A}\mathbf{B}\} = \mathbf{0}$ [23]. The KKT conditions for $(\hat{\mathbf{V}}^\star, \lambda^\star)$ being globally optimal are given by

$$\left(\hat{\mathbf{H}}^H\hat{\mathbf{H}} + \frac{Z+\lambda^\star}{U}\mathbf{I}\right)\hat{\mathbf{V}}^\star = \hat{\mathbf{H}}^H\hat{\mathbf{D}}, \tag{10}$$

$$\|\hat{\mathbf{V}}^\star\|_F^2 - P_{\max} \le 0, \tag{11}$$

$$\lambda^\star \ge 0, \tag{12}$$

$$\lambda^\star(\|\hat{\mathbf{V}}^\star\|_F^2 - P_{\max}) = 0 \tag{13}$$

where (10) is derived by letting (9) equal to $\mathbf{0}$. We obtain the optimal solution based on (10)-(13). Note that, by (6), the virtual queue is nonnegative, *i.e.,* $Z \ge 0$. We derive the optimal solution which is separately discussed in the following cases.

1) $Z + \lambda^\star > 0$*:* From (10), $\hat{\mathbf{H}}^H\hat{\mathbf{H}} + \frac{Z+\lambda^\star}{U}\mathbf{I} \succ \mathbf{0}$ which is invertible, and we have

$$\hat{\mathbf{V}}^\star = \left(\hat{\mathbf{H}}^H\hat{\mathbf{H}} + \frac{Z+\lambda^\star}{U}\mathbf{I}\right)^{-1}\hat{\mathbf{H}}^H\hat{\mathbf{D}}. \tag{14}$$

Depending on Z, $\hat{\mathbf{V}}^\star$ in (14) can be further categorized in two subcases: 1.i) If $Z > 0$: By (11) and (13), if $\|(\hat{\mathbf{H}}^H\hat{\mathbf{H}} + \frac{Z}{U}\mathbf{I})^{-1}\hat{\mathbf{H}}^H\hat{\mathbf{D}}\|_F^2 \le P_{\max}$, then $\lambda^\star = 0$; Otherwise, we have $\lambda^\star > 0$ such that $\|(\hat{\mathbf{H}}^H\hat{\mathbf{H}} + \frac{Z+\lambda^\star}{U}\mathbf{I})^{-1}\hat{\mathbf{H}}^H\hat{\mathbf{D}}\|_F^2 = P_{\max}$. 1.ii) If $Z = 0$: It follows that $\lambda^\star > 0$. By (13), we have $\lambda^\star > 0$ such that $\|(\hat{\mathbf{H}}^H\hat{\mathbf{H}} + \frac{\lambda^\star}{U}\mathbf{I})^{-1}\hat{\mathbf{H}}^H\hat{\mathbf{D}}\|_F^2 = P_{\max}$.

2) $Z = \lambda^\star = 0$: From (10), the optimal solution must satisfy

$$\hat{\mathbf{H}}^H \hat{\mathbf{H}} \hat{\mathbf{V}}^\star = \hat{\mathbf{H}}^H \hat{\mathbf{D}}. \tag{15}$$

We categorize (15) in two subcases: 2.i) If $K < N$: $\hat{\mathbf{H}}^H \hat{\mathbf{H}} \in \mathbb{C}^{N \times N}$ is a rank deficient matrix, and there are infinitely many solutions to $\hat{\mathbf{V}}^\star$. We choose $\hat{\mathbf{V}}^\star$ that minimizes $\|\hat{\mathbf{V}}^\star\|_F^2$ subject to (15), which is an under-determined least square problem with a closed-form solution:

$$\hat{\mathbf{V}}^\star = \hat{\mathbf{H}}^H \left(\hat{\mathbf{H}} \hat{\mathbf{H}}^H\right)^{-1} \hat{\mathbf{D}}. \tag{16}$$

Substitute the above into (11). If $\|\hat{\mathbf{H}}^H (\hat{\mathbf{H}} \hat{\mathbf{H}}^H)^{-1} \hat{\mathbf{D}}\|_F^2 \leq P_{\max}$, then $\hat{\mathbf{V}}^\star$ in (16) is the optimal solution. 2.ii) If $K \geq N$: $\hat{\mathbf{H}}^H \hat{\mathbf{H}} \in \mathbb{C}^{N \times N}$ is of full rank[2], and we have a unique solution:

$$\hat{\mathbf{V}}^\star = \left(\hat{\mathbf{H}}^H \hat{\mathbf{H}}\right)^{-1} \hat{\mathbf{H}}^H \hat{\mathbf{D}}. \tag{17}$$

Again, by (11), if $\|(\hat{\mathbf{H}}^H \hat{\mathbf{H}})^{-1} \hat{\mathbf{H}}^H \hat{\mathbf{D}}\|_F^2 \leq P_{\max}$, then $\hat{\mathbf{V}}^\star$ in (17) is the optimal solution. For both subcases 2.i) and 2.ii), $\hat{\mathbf{V}}^\star$ in (16) or (17) cannot satisfy (11), which means the condition in Case 2) does not hold at optimality, *i.e.,* $\lambda^\star > 0$, and the optimal solution is given by Case 1).

From the above discussion, if at optimality $\lambda^\star = 0$, we have a closed-form solution for $\hat{\mathbf{V}}^\star$ in (16) or (17). Otherwise, we have a semi-closed-form solution for $\hat{\mathbf{V}}^\star$ in (14), where $\lambda^\star > 0$ can be obtained by a bi-section search to ensure the transmit power meets $P_{\max}$ in (11). The computational complexity for calculating $\hat{\mathbf{V}}^\star$ is dominated by the matrix inversion, and thus is in the order of $\mathcal{O}(N^3)$.

V. Performance Bounds

Different from existing works on non-virtualized wireless networks such as [20], in our MIMO WNV system, the impact of imperfect CSI is two-fold on both the InP and the SPs. Therefore, in this section, we develop new techniques to derive the performance bounds for our online algorithm.

We first show in the following lemma that in Algorithm 1, the virtual queue $Z(t)$ is upper bounded at each time t.

Lemma 2. By Algorithm 1, $Z(t)$ satisfies

$$Z(t) \leq U\xi B^2 (1+\delta)^2 + P_{\max} - \bar{P}, \quad \forall t \tag{18}$$

where $\xi \triangleq \sqrt{\frac{N \sum_{m \in \mathcal{M}} P_m}{\bar{P}}}$.

Proof: We omit time index t for notation simplicity in the proof. Let $\hat{\mathbf{H}}^H \hat{\mathbf{H}} = \hat{\mathbf{U}} \hat{\mathbf{\Sigma}} \hat{\mathbf{U}}^H$, where $\hat{\mathbf{U}}$ is an unitary matrix, and $\hat{\mathbf{\Sigma}} = \mathrm{diag}(\hat{\sigma}_1, \ldots, \hat{\sigma}_N)$. It follows that $\hat{\mathbf{H}}^H \hat{\mathbf{H}} + \frac{Z+\lambda^\star}{U} \mathbf{I} = \hat{\mathbf{U}} \hat{\mathbf{\Sigma}}' \hat{\mathbf{U}}^H$, where $\hat{\mathbf{\Sigma}}' = \mathrm{diag}(\hat{\sigma}'_1, \ldots, \hat{\sigma}'_N)$ and $\hat{\sigma}'_n = \hat{\sigma}_n + \frac{Z+\lambda^\star}{U}, \forall n \in \mathcal{N}$. If $Z > 0$, $\hat{\mathbf{V}}^\star$ is given in (14), and we have

$$\|\hat{\mathbf{V}}^\star\|_F \leq \left\|\hat{\mathbf{U}} \hat{\mathbf{\Sigma}}'^{-1} \hat{\mathbf{U}}^H\right\|_F \|\hat{\mathbf{H}}\|_F \|\hat{\mathbf{D}}\|_F \overset{(a)}{\leq} \frac{U}{Z} \sqrt{N} \|\hat{\mathbf{H}}\|_F \|\hat{\mathbf{D}}\|_F$$
$$\overset{(b)}{\leq} \frac{U}{Z} B^2 (1+\delta)^2 \sqrt{N \sum_{m \in \mathcal{M}} P_m} \tag{19}$$

where (a) follows from $\hat{\sigma}_n \geq 0, \forall n \in \mathcal{N}$ and $\lambda^\star \geq 0$, such that $\|\hat{\mathbf{U}} \hat{\mathbf{\Sigma}}'^{-1} \hat{\mathbf{U}}^H\|_F^2 = \mathrm{tr}\left\{\hat{\mathbf{\Sigma}}'^{-2}\right\} = \sum_{n \in \mathcal{N}} \hat{\sigma}'^{-2}_n \leq N \frac{U^2}{Z^2}$, and (b) follows from (5), $\|\hat{\mathbf{W}}_m\|_F^2 \leq P_m, \forall m \in \mathcal{M}$, and

$$\|\hat{\mathbf{D}}\|_F^2 \leq \sum_{m \in \mathcal{M}} \|\hat{\mathbf{H}}_m\|_F^2 \|\hat{\mathbf{W}}_m\|_F^2. \tag{20}$$

From (19), we have the sufficient condition for $Z(t)$ to ensure $\|\hat{\mathbf{V}}^\star(t)\|_F^2 \leq \bar{P}$ for any time t:

$$Z(t) \geq U\xi B^2 (1+\delta)^2. \tag{21}$$

If (21) holds, $\|\hat{\mathbf{V}}^\star(t)\|_F^2 \leq \bar{P}$, and by (6), the virtual queue decreases, *i.e.,* $Z(t+1) \leq Z(t)$. Otherwise, the maximum increase of the virtual queue is $P_{\max} - \bar{P}$, *i.e.,* $Z(t+1) \leq Z(t) + P_{\max} - \bar{P}$. Thus, the virtual queue is upper bounded as in (18) at any time $t \geq 0$. ∎

Note that Algorithm 1 and the upper bound on the virtual queue in Lemma 2 are applicable to any precoding schemes adopted by the SPs. In the following, we consider two common precoding schemes, maximum ratio transmission (MRT) and zero forcing (ZF) precoding. We assume M' SPs adopt MRT precoding and the other SPs adopt ZF precoding. The analysis can be extended to other precoding schemes as well.

Specifically, let $\mathcal{M}' = \{1, \ldots, M'\}$ be the set of SPs that adopt MRT precoding. Each SP $m \in \mathcal{M}'$ uses the following MRT precoding matrix to maximize the received signal-to-noise ratio (SNR) given by

$$\hat{\mathbf{W}}_m^{\text{MRT}}(t) = \sqrt{\frac{P_m}{\|\hat{\mathbf{H}}_m(t)\|_F^2}} \hat{\mathbf{H}}_m^H(t). \tag{22}$$

Each SP $m \in \mathcal{M} \backslash \mathcal{M}'$ adopts ZF precoding to null the inter-user interference, where we assume $K_m \leq N$ in order to perform ZF precoding given by

$$\hat{\mathbf{W}}_m^{\text{ZF}}(t) = \sqrt{\frac{P_m}{\mathrm{tr}\{(\hat{\mathbf{H}}_m(t) \hat{\mathbf{H}}_m^H(t))^{-1}\}}} \hat{\mathbf{H}}_m^H(t) \left(\hat{\mathbf{H}}_m(t) \hat{\mathbf{H}}_m^H(t)\right)^{-1}. \tag{23}$$

Let $\hat{\mathbf{H}}_m(t) \hat{\mathbf{H}}_m^H(t) = \hat{\mathbf{Q}}_m(t) \hat{\mathbf{\Omega}}_m(t) \hat{\mathbf{Q}}_m^H(t)$ where $\hat{\mathbf{Q}}_m(t)$ is a unitary matrix and $\hat{\mathbf{\Omega}}_m(t) = \mathrm{diag}\{\hat{\omega}_{m,1}(t), \ldots, \hat{\omega}_{m,K_m}(t)\}$. Let $\mathbf{D}(t)$ and $\hat{\mathbf{D}}(t)$ be the corresponding virtualization demands under accurate and inaccurate channel state, respectively, according to each SP's precoding scheme in (22) or (23). Below we show that given the CSI inaccuracy δ in (4), there is an upper bound $O(\delta)$ on the deviation between the accurate and inaccurate virtualization demands $\|\mathbf{D}(t) - \hat{\mathbf{D}}(t)\|_F$, for any time t. Note that the impact of inaccurate CSI on the SPs' virtualization demand under MIMO WNV has not been studied in the literature.

Lemma 3. At each time t, the following hold:

$$\|\mathbf{D}(t) - \hat{\mathbf{D}}(t)\|_F \leq \eta B \delta, \tag{24}$$

$$\|\mathbf{D}(t)\|_F \leq \zeta B, \tag{25}$$

$$\|\hat{\mathbf{D}}(t)\|_F \leq \zeta B (1+\delta) \tag{26}$$

[2]Since the channels from BS to users are assumed independent, $\mathbf{H}(t) \in \mathbb{C}^{K \times N}$ is of full rank at each time t. The independent channel assumption is typically satisfied in practice for users at different locations.

where $\eta \triangleq \sqrt{\sum_{m\in\mathcal{M}'}\left(1+\frac{(2+\delta)B}{\hat{B}_m^{\min}}\right)^2 P_m+\sum_{m\in\mathcal{M}\backslash\mathcal{M}'}\left(\frac{B^4(1+\delta)^2}{K_m\hat{\omega}_m^{\min}\omega_m^{\min}}\right)^2 P_m}$, $\hat{B}_m^{\min} \triangleq \min\{\|\hat{\mathbf{H}}_m(t)\|_F : \forall t\}$, $\hat{\omega}_m^{\min} \triangleq \min\{\hat{\omega}_{m,i}(t) : \forall i \in \mathcal{K}_m, \forall t\}$, $\omega_m^{\min} \triangleq \min\{\omega_{m,i}(t) : \forall i \in \mathcal{K}_m, \forall t\}$ in which $\omega_{m,i}$ is similarly defined as $\hat{\omega}_{m,i}$ for $\mathbf{H}_m(t)$, and $\zeta \triangleq \sqrt{\sum_{m\in\mathcal{M}} P_m}$.

Proof: The proofs of (25) and (26) follow from (20). We now prove (24) and omit time index t for notation simplicity. The square of the left-hand side of (24) is given by

$$\|\mathbf{D}-\hat{\mathbf{D}}\|_F^2 = \sum_{m\in\mathcal{M}} \|\mathbf{H}_m\mathbf{W}_m - \hat{\mathbf{H}}_m\hat{\mathbf{W}}_m\|_F^2. \tag{27}$$

For SP $m \in \mathcal{M}'$, by (22), we have

$$\begin{aligned}
&\|\mathbf{H}_m\mathbf{W}_m^{\text{MRT}} - \hat{\mathbf{H}}_m\hat{\mathbf{W}}_m^{\text{MRT}}\|_F \\
&= \sqrt{P_m}\left\|\frac{\mathbf{H}_m\mathbf{H}_m^H}{\|\mathbf{H}_m\|_F} - \frac{\hat{\mathbf{H}}_m\hat{\mathbf{H}}_m^H}{\|\hat{\mathbf{H}}_m\|_F}\right\|_F \\
&= \sqrt{P_m}\left\|\frac{\mathbf{H}_m\mathbf{H}_m^H}{\|\mathbf{H}_m\|_F} - \frac{(\mathbf{H}_m-\tilde{\mathbf{H}}_m)(\mathbf{H}_m^H-\tilde{\mathbf{H}}_m^H)}{\|\mathbf{H}_m-\tilde{\mathbf{H}}_m\|_F}\right\|_F \\
&= \sqrt{P_m}\left\|\left(\frac{\mathbf{H}_m\mathbf{H}_m^H}{\|\mathbf{H}_m\|_F} - \frac{\mathbf{H}_m\mathbf{H}_m^H}{\|\mathbf{H}_m-\tilde{\mathbf{H}}_m\|_F}\right)\right. \\
&\quad \left. - \frac{\tilde{\mathbf{H}}_m\tilde{\mathbf{H}}_m^H - 2\Re\{\tilde{\mathbf{H}}_m\mathbf{H}_m^H\}}{\|\mathbf{H}_m-\tilde{\mathbf{H}}_m\|_F}\right\|_F \\
&\le \sqrt{P_m}\left[\frac{\|\mathbf{H}_m\mathbf{H}_m^H\|_F}{\|\mathbf{H}_m\|_F}\left(1-\frac{\|\mathbf{H}_m\|_F}{\|\mathbf{H}_m-\tilde{\mathbf{H}}_m\|_F}\right)\right. \\
&\quad \left. + \frac{\|\tilde{\mathbf{H}}_m\tilde{\mathbf{H}}_m^H - 2\Re\{\tilde{\mathbf{H}}_m\mathbf{H}_m^H\}\|_F}{\|\mathbf{H}_m-\tilde{\mathbf{H}}_m\|_F}\right] \\
&\overset{(a)}{\le} \sqrt{P_m}\left(B\delta + \frac{\|\tilde{\mathbf{H}}_m\tilde{\mathbf{H}}_m^H - 2\Re\{\tilde{\mathbf{H}}_m\mathbf{H}_m^H\}\|_F}{\|\mathbf{H}_m-\tilde{\mathbf{H}}_m\|_F}\right) \\
&\overset{(b)}{\le} \sqrt{P_m}B\delta\left(1+\frac{(2+\delta)B}{\|\hat{\mathbf{H}}_m\|_F}\right) \le \sqrt{P_m}B\delta\left(1+\frac{(2+\delta)B}{\hat{B}_m^{\min}}\right)
\end{aligned} \tag{28}$$

where (a) is because

$$\frac{\|\mathbf{H}_m\mathbf{H}_m^H\|_F}{\|\mathbf{H}_m\|_F}\left(1-\frac{\|\mathbf{H}_m\|_F}{\|\mathbf{H}_m-\tilde{\mathbf{H}}_m\|_F}\right) \le B\left(1-\frac{1}{1+\delta}\right) \le B\delta,$$

and (b) follows from

$$\begin{aligned}
&\|\tilde{\mathbf{H}}_m\tilde{\mathbf{H}}_m^H - 2\Re\{\tilde{\mathbf{H}}_m\mathbf{H}_m^H\}\|_F \le \|\tilde{\mathbf{H}}_m\tilde{\mathbf{H}}_m^H\|_F + 2\|\tilde{\mathbf{H}}_m\mathbf{H}_m^H\|_F \\
&\le \|\tilde{\mathbf{H}}_m\|_F^2 + 2\|\tilde{\mathbf{H}}_m\|_F\|\mathbf{H}_m\|_F \le B^2\delta^2 + 2B^2\delta \le (2+\delta)B^2\delta.
\end{aligned}$$

For SP $m \in \mathcal{M}\backslash\mathcal{M}'$, by (23), we have

$$\begin{aligned}
&\|\mathbf{H}_m\mathbf{W}_m^{\text{ZF}} - \hat{\mathbf{H}}_m\hat{\mathbf{W}}_m^{\text{ZF}}\|_F \\
&= \sqrt{P_m}\left\|\frac{\mathbf{I}_{K_m}}{\sqrt{\text{tr}\{(\mathbf{H}_m\mathbf{H}_m^H)^{-1}\}}} - \frac{\mathbf{I}_{K_m}}{\sqrt{\text{tr}\{(\hat{\mathbf{H}}_m\hat{\mathbf{H}}_m^H)^{-1}\}}}\right\|_F \\
&\overset{(a)}{\le} \sqrt{P_m K_m}\frac{\left|\sqrt{\text{tr}\{\hat{\mathbf{\Omega}}_m^{-1}\}} - \sqrt{\text{tr}\{\mathbf{\Omega}_m^{-1}\}}\right|}{\frac{K_m}{B^2(1+\delta)}} \\
&= \sqrt{\frac{P_m}{K_m}}B^2(1+\delta)\frac{\left|\text{tr}\{\hat{\mathbf{\Omega}}_m^{-1} - \mathbf{\Omega}_m^{-1}\}\right|}{\sqrt{\text{tr}\{\hat{\mathbf{\Omega}}_m^{-1}\}} + \sqrt{\text{tr}\{\mathbf{\Omega}_m^{-1}\}}} \\
&\overset{(b)}{\le} \sqrt{\frac{P_m}{K_m}}B^2(1+\delta)\frac{B^2(2+\delta)\delta}{\hat{\omega}_m^{\min}\omega_m^{\min}\frac{(2+\delta)\sqrt{K_m}}{B(1+\delta)}} \le \frac{\sqrt{P_m}B^5(1+\delta)^2\delta}{K_m\hat{\omega}_m^{\min}\omega_m^{\min}}
\end{aligned} \tag{29}$$

where (a) follows from $\text{tr}\{(\hat{\mathbf{H}}_m\hat{\mathbf{H}}_m^H)^{-1}\} = \text{tr}\{\hat{\mathbf{\Omega}}_m^{-1}\} = \sum_{i\in\mathcal{K}_m}\hat{\omega}_{m,i}^{-1} \ge \frac{K_m}{B^2(1+\delta)^2}$, (b) follows from $\sqrt{\text{tr}\{\hat{\mathbf{\Omega}}_m^{-1}\}} + \sqrt{\text{tr}\{\mathbf{\Omega}_m^{-1}\}} \ge \sqrt{\frac{K_m}{B^2(1+\delta)^2}} + \sqrt{\frac{K_m}{B^2}} = \frac{(2+\delta)\sqrt{K_m}}{B(1+\delta)}$, and

$$\begin{aligned}
&\left|\text{tr}\{\hat{\mathbf{\Omega}}_m^{-1} - \mathbf{\Omega}_m^{-1}\}\right| = \left|\sum_{i\in\mathcal{K}_m}\hat{\omega}_{m,i}^{-1} - \omega_{m,i}^{-1}\right| \\
&\le \frac{\left|\sum_{i\in\mathcal{K}_m}\omega_{m,i} - \hat{\omega}_{m,i}\right|}{\hat{\omega}_m^{\min}\omega_m^{\min}} = \frac{\left|\|\mathbf{H}_m\|_F^2 - \|\hat{\mathbf{H}}_m\|_F^2\right|}{\hat{\omega}_m^{\min}\omega_m^{\min}} \\
&= \frac{(\|\mathbf{H}_m\|_F + \|\hat{\mathbf{H}}_m\|_F)\left|\|\mathbf{H}_m\|_F - \|\hat{\mathbf{H}}_m\|_F\right|}{\hat{\omega}_m^{\min}\omega_m^{\min}} \le \frac{B^2(2+\delta)\delta}{\hat{\omega}_m^{\min}\omega_m^{\min}}.
\end{aligned}$$

Applying inequalities (28) and (29) to (27) yields (24). ■

For channel state $\mathbf{H}(t)$ being i.i.d. over time, there exists a stationary randomized optimal precoding solution $\mathbf{V}_{\text{opt}}(t)$ to **P1**, which depends only on the (unknown) distribution of $\mathbf{H}(t)$, and achieves the minimum objective value of **P1**, denoted by ρ_{opt} [13]. Define $\phi(\mathbf{H}(t),\mathbf{V}(t),\mathbf{D}(t)) \triangleq U\|\mathbf{H}(t)\mathbf{V}(t) - \mathbf{D}(t)\|_F^2 + Z(t)\|\mathbf{V}(t)\|_F^2$, and note that $\phi(\hat{\mathbf{H}}(t),\hat{\mathbf{V}}(t),\hat{\mathbf{D}}(t))$ is the objective function in **P2**. Leveraging the results in Lemma 3, we now show in the following lemma that, at each time t, for a given CSI inaccuracy δ in (4), there exists an upper bound $O(\delta)$ on $\phi(\mathbf{H}(t),\hat{\mathbf{V}}^\star(t),\mathbf{D}(t)) - \phi(\mathbf{H}(t),\mathbf{V}_{\text{opt}}(t),\mathbf{D}(t))$, which is the performance gap between using the optimal solution $\hat{\mathbf{V}}^\star(t)$ to **P2** under the inaccurate channel state $\hat{\mathbf{H}}(t)$ and using the optimal solution $\mathbf{V}_{\text{opt}}(t)$ to **P1** under the accurate channel state $\mathbf{H}(t)$. We point out that, different from [20], our proof explicitly considers the two-fold impact of CSI inaccuracy on both InP and SPs under MIMO WNV.

Lemma 4. At each time t, the following holds:

$$\phi(\mathbf{H}(t),\hat{\mathbf{V}}^\star(t),\mathbf{D}(t)) - \phi(\mathbf{H}(t),\mathbf{V}_{\text{opt}}(t),\mathbf{D}(t)) \le U\varphi \tag{30}$$

where

$$\varphi \triangleq 2\Big[(2+\delta)(P_{\max}+\zeta\eta)+2(\zeta(1+\delta)+\eta)\sqrt{P_{\max}}\Big]B^2\delta = O(\delta).$$

Proof: We omit time index t for notation simplicity. The proof of (30) consists of five steps as follows.

Step 1: From the first order condition of real-valued scalar convex function $\phi(\mathbf{H},\hat{\mathbf{V}}^\star,\mathbf{D})$ with respect to the complex-valued matrix variable $\mathbf{D}$ [24], we have

$$\begin{aligned}
&\phi(\mathbf{H},\hat{\mathbf{V}}^\star,\mathbf{D}) - \phi(\mathbf{H},\hat{\mathbf{V}}^\star,\hat{\mathbf{D}}) \\
&\le -2\Re\{\text{tr}\{\nabla_{\mathbf{D}^*}\phi(\mathbf{H},\hat{\mathbf{V}}^\star,\mathbf{D})^H(\hat{\mathbf{D}}-\mathbf{D})\}\} \\
&\overset{(a)}{=} 2U\Re\{\text{tr}\{(\mathbf{H}\hat{\mathbf{V}}^\star - \mathbf{D})^H(\hat{\mathbf{D}}-\mathbf{D})\}\}
\end{aligned}$$

$$
\begin{aligned}
&\leq 2U|\operatorname{tr}\{(\mathbf{H}\hat{\mathbf{V}}^{\star}-\mathbf{D})^{H}(\hat{\mathbf{D}}-\mathbf{D})\}| \\
&\leq 2U\|\mathbf{H}\hat{\mathbf{V}}^{\star}-\mathbf{D}\|_{F}\|\hat{\mathbf{D}}-\mathbf{D}\|_{F} \\
&\leq 2U(\|\mathbf{H}\|_{F}\|\hat{\mathbf{V}}^{\star}\|_{F}+\|\mathbf{D}\|_{F})\|\hat{\mathbf{D}}-\mathbf{D}\|_{F} \\
&\overset{(b)}{\leq} 2U(\sqrt{P_{\max}}+\zeta)\eta B^{2}\delta
\end{aligned} \tag{31}
$$

where (a) follows from $\nabla_{\mathbf{D}^*}\phi(\mathbf{H},\hat{\mathbf{V}}^{\star},\mathbf{D})= -U(\mathbf{H}\hat{\mathbf{V}}^{\star}-\mathbf{D})$, and (b) follows from (1), (8), (24), and (25).

Step 2: From the first order condition of real-valued scalar convex function $\phi(\mathbf{H},\hat{\mathbf{V}}^{\star},\hat{\mathbf{D}})$ with respect to the complex-valued matrix variable $\mathbf{H}$, we have

$$
\begin{aligned}
&\phi(\mathbf{H},\hat{\mathbf{V}}^{\star},\hat{\mathbf{D}})-\phi(\hat{\mathbf{H}},\hat{\mathbf{V}}^{\star},\hat{\mathbf{D}}) \\
&\leq -2\Re\{\operatorname{tr}\{\nabla_{\mathbf{H}^*}\phi(\mathbf{H},\hat{\mathbf{V}}^{\star},\hat{\mathbf{D}})^{H}(\hat{\mathbf{H}}-\mathbf{H})\}\} \\
&\overset{(a)}{=} 2U\Re\{\operatorname{tr}\{(\mathbf{H}\hat{\mathbf{V}}^{\star}\hat{\mathbf{V}}^{\star H}-\hat{\mathbf{D}}\hat{\mathbf{V}}^{\star H})^{H}(\mathbf{H}-\hat{\mathbf{H}})\}\} \\
&\leq 2U(\|\mathbf{H}\|_{F}\|\hat{\mathbf{V}}^{\star}\|_{F}+\|\hat{\mathbf{D}}\|_{F})\|\hat{\mathbf{V}}^{\star}\|_{F}\|\mathbf{H}-\hat{\mathbf{H}}\|_{F} \\
&\overset{(b)}{\leq} 2U\left[P_{\max}+\zeta(1+\delta)\sqrt{P_{\max}}\right]B^{2}\delta
\end{aligned} \tag{32}
$$

where (a) follows from $\nabla_{\mathbf{H}^*}\phi(\mathbf{H},\hat{\mathbf{V}}^{\star},\hat{\mathbf{D}}) = U(\mathbf{H}\hat{\mathbf{V}}^{\star}\hat{\mathbf{V}}^{\star H} - \hat{\mathbf{D}}\hat{\mathbf{V}}^{\star H})$, and (b) follows from (1), (4), (8), and (26).

Step 3: In Algorithm 1, $\hat{\mathbf{V}}^{\star}$ is the optimal precoding matrix that minimizes $\phi(\hat{\mathbf{H}},\hat{\mathbf{V}},\hat{\mathbf{D}})$ as the objective in **P2** over all the precoding policies including $\mathbf{V}_{\text{opt}}$, it follows that

$$
\phi(\hat{\mathbf{H}},\hat{\mathbf{V}}^{\star},\hat{\mathbf{D}})-\phi(\hat{\mathbf{H}},\mathbf{V}_{\text{opt}},\hat{\mathbf{D}})\leq 0. \tag{33}
$$

Step 4: Similarly to Step 2, we have

$$
\begin{aligned}
&\phi(\hat{\mathbf{H}},\mathbf{V}_{\text{opt}},\hat{\mathbf{D}})-\phi(\mathbf{H},\mathbf{V}_{\text{opt}},\hat{\mathbf{D}}) \\
&\leq 2U(P_{\max}+\zeta\sqrt{P_{\max}})(1+\delta)B^{2}\delta.
\end{aligned} \tag{34}
$$

Step 5: Similarly to Step 1, we have

$$
\begin{aligned}
&\phi(\mathbf{H},\mathbf{V}_{\text{opt}},\hat{\mathbf{D}})-\phi(\mathbf{H},\mathbf{V}_{\text{opt}},\mathbf{D}) \\
&\leq 2U\left[\sqrt{P_{\max}}+\zeta(1+\delta)\right]\eta B^{2}\delta.
\end{aligned} \tag{35}
$$

Summing over (31)-(35) yields (30). ∎

Leveraging the key results in Lemma 4, we show that the expected DPP metric over the virtual queue $Z(t)$ under the accurate channel state $\mathbf{H}(t)$ using the optimal precoding solution $\hat{\mathbf{V}}^{\star}(t)$ to **P2** is upper bounded at each time t. The technique used in the proof is similar to Lemma 3 in [20] and hence is omitted.

Lemma 5. At each time t, we have

$$
\begin{aligned}
&\mathbb{E}\{\Delta(t)\}+U\mathbb{E}\{\|\mathbf{H}(t)\hat{\mathbf{V}}^{\star}(t)-\mathbf{D}(t)\|_{F}^{2}\} \\
&\leq U\mathbb{E}\{\|\mathbf{H}(t)\mathbf{V}_{\text{opt}}(t)-\mathbf{D}(t)\|_{F}^{2}\}+U\varphi+S
\end{aligned} \tag{36}
$$

where φ is given in Lemma 4 and S is defined below (7).

Leveraging the results in Lemma 2 and Lemma 5, the following theorem provides performance bounds for Algorithm 1 with imperfect CSI over any given time horizon T. The proof utilizes the Lyapunov optimization techniques [13] and key results in Lemma 2 and Lemma 5. Details are omitted due to space constraint.

Theorem 6. Given any $\epsilon>0$, set $U=\frac{S}{\epsilon}$ in Algorithm 1. For any $T>0$, for $\hat{\mathbf{V}}^{\star}(t)$ produced by Algorithm 1 with $\hat{\mathbf{H}}(t)$, the following hold regardless of the distribution of $\mathbf{H}(t)$:

$$
\frac{1}{T}\sum_{t=0}^{T-1}\mathbb{E}\left\{\|\mathbf{H}(t)\hat{\mathbf{V}}^{\star}(t)-\mathbf{D}(t)\|_{F}^{2}\right\}\leq \rho_{\text{opt}}+\varphi+\epsilon, \tag{37}
$$

$$
\frac{1}{T}\sum_{t=0}^{T-1}\|\hat{\mathbf{V}}^{\star}(t)\|_{F}^{2}\leq \bar{P}+\frac{SB^{2}(1+\delta)^{2}\xi+\epsilon(P_{\max}-\bar{P})}{\epsilon T} \tag{38}
$$

where ρ_{opt} is the minimum objective value of **P1** under $\mathbf{H}(t)$, φ is defined below (30), and ξ is defined below (18).

Note that, different from the standard $(\epsilon,\frac{1}{\epsilon})$ trade-off in Lyapunov optimization with accurate system state information [13], Theorem 6 provides an upper bound on the objective value of **P1** in (37), *i.e.,* the time-averaged expected deviation of the actual precoding by the InP from the virtualization demand under inaccurate channel state. It indicates that, for any given T, the performance of Algorithm 1 using inaccurate channel state $\hat{\mathbf{H}}(t)$ can be arbitrarily close to the optimum achieved with accurate channel state $\mathbf{H}(t)$ plus $O(\delta)$, where the performance gap ϵ is a controllable parameter by our design and can be set arbitrarily small. Furthermore, (38) provides a bound on the time-averaged transmit power for any given T. The bound indicates that for all $T\geq\frac{1}{\epsilon^2}$, Algorithm 1 guarantees that the deviation from the long-term transmit power limit $\bar{P}$ is within $O(\epsilon)$. In particular, as $T\to\infty$, (38) becomes the long-term average transmit power constraint (2).

VI. Simulation Results

In this section, we present extensive simulation results under typical urban micro-cell LTE network settings. We study the impact of various system parameters on algorithm convergence and performance. For performance comparison, it has already been demonstrated in [11] that the spatial isolation approach used in this work substantially outperforms the physical isolation approach used in other existing MIMO WNV studies [4]-[9], in terms of throughput and energy consumption. Indeed, the physical isolation approach, in exchange for achieving network virtualization, suffers performance loss in comparison with a non-virtualized system. Therefore, we will focus on demonstrating that our spatial isolation approach compares favorably against a non-virtualized system.

A. Simulation Setup

We consider an InP that owns a BS equipped with $N=30$ antennas at the center of an urban hexagon micro-cell of 500 m radius. The InP serves $M=4$ SPs. Each SP serves 2 to 5 users uniformly distributed in the cell. Following the typical LTE specifications [25], we set $P_{\max}=16$ dBm, noise power spectral density $N_0=-174$ dBm/Hz, noise figure $N_F=10$ dB, and we focus on the channel over one subcarrier with bandwidth $B_W=10$ kHz as default system parameters. The fading channel from the BS to user k is modeled as $\mathbf{h}_k=\sqrt{\beta_k}\mathbf{g}_k$, where $\mathbf{g}_k\sim\mathcal{CN}(\mathbf{0},\mathbf{I})$, $\beta_k[\text{dB}]=-31.54-33\log_{10}(d_k)-\psi_k$ represents the path-loss

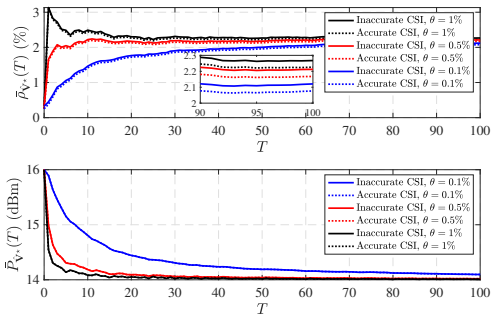

(a) All SPs adopt MRT precoding.

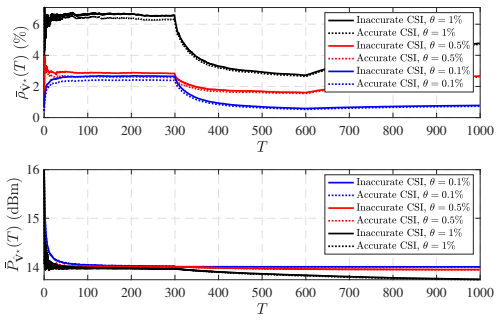

(b) One half of the SPs adopt MRT precoding and the other half of the SPs adopt ZF precoding. Channel distribution changes at the 300th and 600th time slots.

Fig. 2. $\bar{\rho}_{\hat{\mathbf{V}}^\star}(T)$ and $\bar{P}_{\hat{\mathbf{V}}^\star}(T)$ vs. T under different θ.

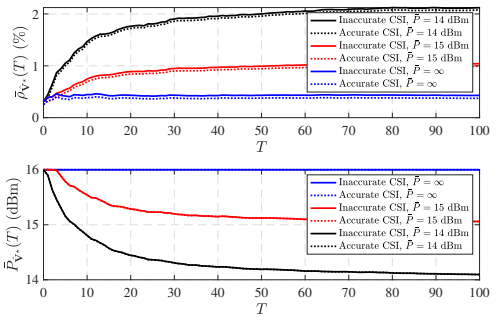

(a) All SPs adopt MRT precoding.

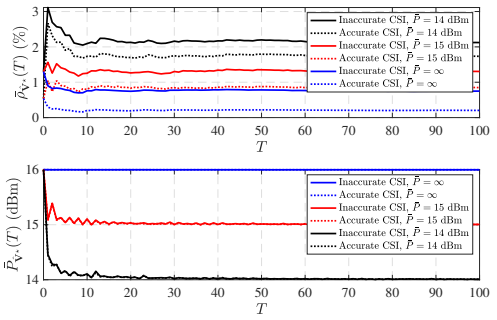

(b) All SPs adopt ZF precoding.

Fig. 3. $\bar{\rho}_{\hat{\mathbf{V}}^\star}(T)$ and $\bar{P}_{\hat{\mathbf{V}}^\star}(T)$ vs. T under different $\bar{P}$.

and shadowing, with d_k being the distance in kilometers from the BS to user k and $\psi_k \sim \mathcal{CN}(0, \sigma_\phi^2)$ being the shadowing with $\sigma_\phi = 8$ dB.

We assume the time-division duplex mode, where the channel estimation is performed over the uplink channel. The BS estimates each channel through L pilot symbols with a given power P_{pilot}. We set $L = 1$, $P_{\text{pilot}} = 10$ dBm as default, and assume the minimum mean-square error channel estimation, with error $\mathbf{e}_k = \mathbf{h}_k - \hat{\mathbf{h}}_k$ where $\mathbf{e}_k$ is Gaussian distributed with covariance $\mathbf{C}_{\mathbf{e}_k} = \mathbf{C}_{\mathbf{h}_k} - \mathbf{C}_{\mathbf{h}_k}\mathbf{T}^H(\mathbf{T}\mathbf{C}_{\mathbf{h}_k}\mathbf{T}^H + \sigma_n^2\mathbf{I})^{-1}\mathbf{T}\mathbf{C}_{\mathbf{h}_k}$, in which $\mathbf{C}_{\mathbf{h}_k} \triangleq \mathbb{E}\{\mathbf{h}_k\mathbf{h}_k^H\}$, $\mathbf{T} \triangleq \sqrt{P_{\text{pilot}}}[\mathbf{I}, \ldots, \mathbf{I}]^H$, and $\sigma_n^2 = N_0 B_W + N_F$ is the noise power [26]. We define the time-averaged normalized CSI inaccuracy as $\bar{e}_{\mathbf{H}} \triangleq \frac{1}{T}\sum_{t=0}^{T-1} \frac{\|\tilde{\mathbf{H}}(t)\|_F}{\|\mathbf{H}(t)\|_F}$.

To study the performance of Algorithm 1, we define the normalized time-averaged precoding deviation from the virtualization demand as

$$\bar{\rho}_{\hat{\mathbf{V}}^\star}(T) \triangleq \frac{\frac{1}{T}\sum_{t=0}^{T-1} \|\mathbf{H}(t)\hat{\mathbf{V}}^\star(t) - \mathbf{D}(t)\|_F^2}{\frac{1}{T}\sum_{t=0}^{T-1} \|\mathbf{D}(t)\|_F^2} \tag{39}$$

and the time-averaged downlink transmit power as

$$\bar{P}_{\hat{\mathbf{V}}^\star}(T) \triangleq \frac{1}{T}\sum_{t=0}^{T-1} \|\hat{\mathbf{V}}^\star(t)\|_F^2.$$

We assume that the InP allocates the transmit power $P_m = \frac{P_{\max}}{M}$ to each SP m such that $\sum_{m\in\mathcal{M}} P_m = P_{\max}$.

For $\bar{\rho}_{\hat{\mathbf{V}}^\star}(T)$ in (39), $\|\mathbf{D}(t)\|_F^2 \le B^2 P_{\max}$ by (25), based on the performance upper bound in (37), we set $\epsilon = \theta B^2 P_{\max}$ where θ is used as a controllable parameter. We set $B = 1.645\sqrt{N\sum_{k\in\mathcal{K}}\beta_k}$, which gives a Chernoff upper bound of 3.8×10^{-9} for the probability of bound violation $\mathbb{P}\{\|\mathbf{H}(t)\|_F > B\}$.

B. Effect of Weighting Factor U

We first study the effect of weighting factor $U = \frac{S}{\epsilon}$ on the performance by varying ϵ through θ. Fig. 2(a) shows the time trajectory of $\bar{\rho}_{\hat{\mathbf{V}}^\star}(T)$ and $\bar{P}_{\hat{\mathbf{V}}^\star}(T)$ under different values of θ, for $\bar{P} = 14$ dBm and $\bar{e}_{\mathbf{H}} = 5.7\%$, when all SPs adopt MRT precoding. Fast convergence of the proposed algorithm (within 100 time slots) is observed. As θ decreases, U becomes larger, and more emphasis is on the precoding deviation $\hat{\rho}(t)$, and less on the Lyapunov drift $\Delta(t)$ in the DPP metric. As a result, it takes a longer time for the virtual queue to stabilize, and thus the performance to reach the steady state. Furthermore, at convergence, $\bar{\rho}_{\hat{\mathbf{V}}^\star}(T)$ decreases as θ decreasing, and $\bar{P}_{\hat{\mathbf{V}}^\star}(T)$ converges to $\bar{P}$. These are consistent with Theorems 6. Fig. 2(b) shows the algorithm performance under a practical scenario where the SPs are free to adopt either MRT or ZF precoding, and the channel distribution changes over time (*e.g.*, due to mobility). Our proposed algorithm can track the change of channel distribution while limiting $\bar{\rho}_{\hat{\mathbf{V}}^\star}(T)$ under 3% when $\theta = 0.1\%$. As such, we set $\theta = 0.1\%$ as the default value for the rest of simulation.

C. Performance vs. Long-Term Transmit Power Limit $\bar{P}$

Fig. 3 shows the time trajectory of $\bar{\rho}_{\hat{\mathbf{V}}^\star}(T)$ and $\bar{P}_{\hat{\mathbf{V}}^\star}(T)$ under different values of $\bar{P}$, when all SPs adopt either MRT or ZF precoding. The case of $\bar{P} = \infty$ corresponds to removing the long-term average transmit power constraint (2) from **P1**. At steady state, $\bar{\rho}_{\hat{\mathbf{V}}^\star}(T)$ is under 1% when $\bar{P} = \infty$ for both the

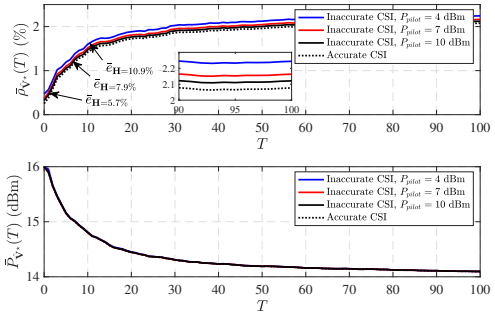

(a) All SPs adopt MRT precoding.

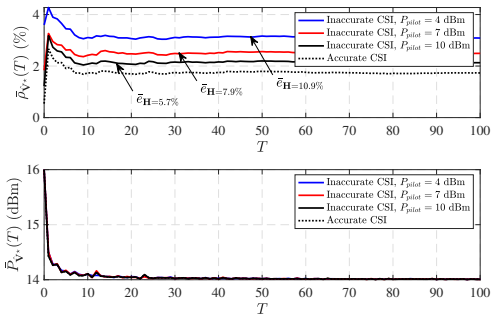

(b) All SPs adopt ZF precoding.

Fig. 4. $\bar{\rho}_{\hat{\mathbf{V}}^\star}(T)$ and $\bar{P}_{\hat{\mathbf{V}}^\star}(T)$ vs. T under different P_{pilot}.

MRT and ZF precoding cases. When $\bar{P} = 14$ dBm, the steady-state value of $\bar{\rho}_{\hat{\mathbf{V}}^\star}(T)$ is only around 2% for both cases. Note that there is a natural trade-off between $\bar{P}$ and $\bar{\rho}_{\hat{\mathbf{V}}^\star}(T)$, which allows the InP to balance the transmit power consumption and the deviation of actual precoding from the virtualization demand.

D. Performance vs. CSI Inaccuracy

In Fig. 4, we study the impact of CSI inaccuracy on the performance by varying P_{pilot}. As P_{pilot} decreases from 10 dBm to 4 dBm, $\bar{e}_{\mathbf{H}}$ increases from 5.7% to 10.9%, while the steady-state values of $\bar{\rho}_{\hat{\mathbf{V}}^\star}(T)$ is still under 3% for both precoding schemes. We observe that $\bar{\rho}_{\hat{\mathbf{V}}^\star}(T)$ is more sensitive to $\bar{e}_{\mathbf{H}}$ when all SPs adopt ZF precoding, as compared to the MRT precoding case. The reason is that ZF precoding nulls the inter-user interference and thus its performance is sensitive to CSI inaccuracy. The steady-state value of $\bar{P}_{\hat{\mathbf{V}}^\star}(T)$ is not sensitive to the value of $\bar{e}_{\mathbf{H}}$.

E. Performance Comparison with Non-virtualized Network

We compare the performance between virtualized and non-virtualized networks. For the non-virtualized network, all users share the channel bandwidth B_W. We assume the InP directly serves all users and maximizes the long-term time-averaged expected sum rate subject to both long-term and short-term transmit power constraints through optimizing the transmit power of MRT or ZF precoding as follows:

$$\mathbf{P3}: \quad \min_{\{\hat{\alpha}(t)\}} \quad \lim_{T\to\infty} \frac{1}{T} \sum_{t=0}^{T-1} \mathbb{E}\left\{ -\sum_{k\in\mathcal{K}} \hat{R}_k(t) \right\}$$

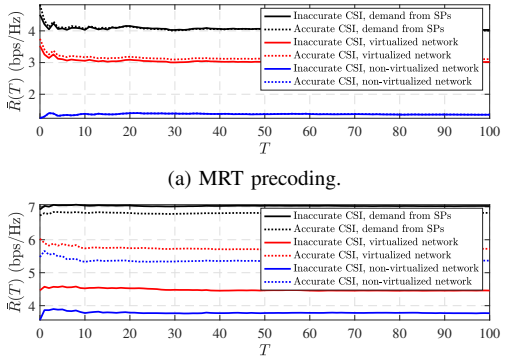

(a) MRT precoding.

(b) ZF precoding.

Fig. 5. Comparison of $\bar{R}(T)$ between virtualized and non-virtualized networks.

$$\text{s.t.} \quad \lim_{T\to\infty} \frac{1}{T} \sum_{t=0}^{T-1} \mathbb{E}\{\|\hat{\alpha}(t)\hat{\mathbf{W}}(t)\|_F^2\} \le \bar{P},$$
$$\|\hat{\alpha}(t)\hat{\mathbf{W}}(t)\|_F^2 \le P_{\max}$$

where $\hat{R}_k(t) = \log_2\left(1+\frac{\hat{\alpha}^2(t)|\hat{\mathbf{h}}_k^T(t)\hat{\mathbf{w}}_k(t)|^2}{\hat{\alpha}^2(t)\sum_{k'\in\mathcal{K},k'\neq k}|\hat{\mathbf{h}}_k^T(t)\hat{\mathbf{w}}_{k'}(t)|^2+\sigma_n^2}\right)$, $\hat{\mathbf{W}}(t) = \hat{\mathbf{H}}^H(t)$ if the InP adopts MRT precoding, and $\hat{\mathbf{W}}(t) = \hat{\mathbf{H}}^H(t)(\hat{\mathbf{H}}(t)\hat{\mathbf{H}}^H(t))^{-1}$ if the InP adopts ZF precoding. The solution to **P3** is omitted due to space constraints.

Fig. 5 shows the time-averaged per-user rate defined as $\bar{R}(T) \triangleq \frac{1}{TK}\sum_{t=0}^{T-1}\sum_{k\in\mathcal{K}}\log_2\left(1+\frac{|\mathbf{h}_k^T(t)\hat{\mathbf{v}}_k(t)|^2}{\sum_{k'\in\mathcal{K},k'\neq k}|\mathbf{h}_k^T(t)\hat{\mathbf{v}}_{k'}(t)|^2+\sigma_n^2}\right)$ achieved by the virtualized network and non-virtualized networks with $\bar{P} = 15$ dBm. We consider two cases of MRT and ZF precoding. Note that the per-user rate demand from the SPs at each time t is calculated by $\frac{1}{K}\sum_{m\in\mathcal{M}}\sum_{k\in\mathcal{K}_m}\log_2\left(1+\frac{|\hat{\mathbf{h}}_{m,k}^T(t)\hat{\mathbf{w}}_{m,k}(t)|^2}{\sum_{k'\in\mathcal{K}_m,k'\neq k}|\hat{\mathbf{h}}_{m,k}^T(t)\hat{\mathbf{w}}_{m,k'}(t)|^2+\sigma_n^2}\right)$. We observe that it is higher than the actual rate achieved, since the SPs request maximum BS transmit power $P_{\max} = 16$ dBm without considering the inter-SP interference.

Compared with the non-virtualized network, a virtualized network using the proposed algorithm achieves a higher rate. This is because our downlink precoding minimizes the precoding deviation, while implicitly reducing the inter-SP interference. This indirectly increases the rates of all SPs.

VII. Conclusions

This paper considers online downlink precoding design for WNV in MIMO fading systems with imperfect CSI. We propose an online MIMO WNV algorithm to minimize the long-term time-averaged expected deviation of the InP's actual precoding solution from the virtualization demand set by the SPs, subject to both long-term and short-term transmit power constraints. Our proposed algorithm only depends on the current imperfect CSI, without knowledge of the channel distribution, and the online precoding solution is in semi-closed form. Our analysis considers the two-fold impact of imperfect CSI on both InP and SPs, to reveal an $O(\delta)$ optimality gap over any given time horizon. Simulation results based on realistic LTE network settings show that the algorithm converges fast and is robust to imperfect CSI.

REFERENCES

[1] C. Liang and F. R. Yu, "Wireless network virtualization: A survey, some research issues and challenges," *IEEE Commun. Surveys Tuts.*, vol. 17, pp. 358–380, 2015.

[2] J. van de Belt, H. Ahmadi, and L. E. Doyle, "Defining and surveying wireless link virtualization and wireless network virtualization," *IEEE Commun. Surveys Tuts.*, vol. 19, pp. 1603–1627, 2017.

[3] M. Richart, J. Baliosian, J. Serrat, and J. Gorricho, "Resource slicing in virtual wireless networks: A survey," *IEEE Trans. Netw. Service Manag.*, vol. 13, pp. 462–476, Sep. 2016.

[4] V. Jumba, S. Parsaeefard, M. Derakhshani, and T. Le-Ngoc, "Resource provisioning in wireless virtualized networks via massive-MIMO," *IEEE Wireless Commun. Lett.*, vol. 4, pp. 237–240, Jun. 2015.

[5] Z. Chang, Z. Han, and T. Ristaniemi, "Energy efficient optimization for wireless virtualized small cell networks with large-scale multiple antenna," *IEEE Trans. Commun.*, vol. 65, pp. 1696–1707, Apr. 2017.

[6] K. Zhu and E. Hossain, "Virtualization of 5G cellular networks as a hierarchical combinatorial auction," *IEEE Trans. Mobile Comput.*, vol. 15, pp. 2640–2654, Oct. 2016.

[7] S. Parsaeefard, R. Dawadi, M. Derakhshani, T. Le-Ngoc, and M. Baghani, "Dynamic resource allocation for virtualized wireless networks in massive-MIMO-aided and fronthaul-limited C-RAN," *IEEE Trans. Veh. Technol.*, vol. 66, pp. 9512–9520, Oct. 2017.

[8] D. Tweed and T. Le-Ngoc, "Dynamic resource allocation for uplink MIMO NOMA VWN with imperfect SIC," in *Proc. IEEE Int. Conf. Commun. (ICC)*, May 2018.

[9] Y. Liu, M. Derakhshani, S. Parsaeefard, S. Lambotharan, and K. Wong, "Antenna allocation and pricing in virtualized massive MIMO networks via Stackelberg game," *IEEE Trans. Commun.*, vol. 66, pp. 5220–5234, Nov. 2018.

[10] N. M. Mosharaf Kabir Chowdhury and R. Boutaba, "Network virtualization: state of the art and research challenges," *IEEE Commun. Mag.*, vol. 47, pp. 20–26, Jul. 2009.

[11] M. Soltanizadeh, B. Liang, G. Boudreau, and S. H. Seyedmehdi, "Power minimization in wireless network virtualization with massive MIMO," in *Proc. Intel. Conf. Commun. (ICC) Workshops*, May 2018.

[12] H. Q. Ngo, E. G. Larsson, and T. L. Marzetta, "Energy and spectral efficiency of very large multiuser MIMO systems," *IEEE Trans. Commun.*, vol. 61, pp. 1436–1449, Apr. 2013.

[13] M. J. Neely, *Stochastic Network Optimization with Application on Communication and Queueing Systems*. Morgan & Claypool, 2010.

[14] M. Zinkevich, "Online convex programming and generalized infinitesimal gradient ascent," in *Proc. Int. Conf. Mach. Learn. (ICML)*, 2003, pp. 928–935.

[15] P. Mertikopoulos and E. V. Belmega, "Learning to be green: Robust energy efficiency maximization in dynamic MIMO-OFDM system," *IEEE J. Sel. Areas Commun.*, vol. 34, pp. 743–757, Apr. 2016.

[16] P. Mertikopoulos and A. L. Moustakas, "Learning in an uncertain world: MIMO covariance matrix optimization with imperfect feedback," *IEEE Trans. Signal Process.*, vol. 64, pp. 5–18, Jan. 2016.

[17] F. Amirnavaei and M. Dong, "Online power control optimization for wireless transmission with energy harvesting and storage," *IEEE Trans. Wireless Commun.*, vol. 15, pp. 4888–4901, Jul. 2016.

[18] M. Dong, W. Li, and F. Amirnavaei, "Online joint power control for two-hop wireless relay networks with energy harvesting," *IEEE Trans. Signal Process.*, vol. 66, pp. 463–478, Jan. 2018.

[19] J. Wang, M. Dong, B. Liang, and G. Boudreau, "Online downlink MIMO wireless network virtualization in fading environments," in *Proc. IEEE Global Commun. Conf. (GLOBECOM)*, Dec. 2019.

[20] H. Yu and M. J. Neely, "Dynamic transmit covariance design in MIMO fading systems with unknown channel distributions and inaccurate channel state information," *IEEE Trans. Wireless Commun.*, vol. 16, pp. 3996–4008, Jun. 2017.

[21] D. P. Bertsekas, *Dynamic Programming and Optimal Control*. Athena Scientific, 2007.

[22] S. Boyd and L. Vandenberghe, *Convex Optimization*. Cambridge University Press, 2004.

[23] A. Hjorungnes and D. Gesbert, "Complex-valued matrix differentiation: Techniques and key results," *IEEE Trans. Signal Process.*, vol. 55, pp. 2740–2746, Jun. 2007.

[24] D. H. Brandwood, "A complex gradient operator and its application in adaptive array theory," *IEE Proceedings H - Microwaves, Optics and Antennas*, vol. 130, pp. 11–16, Feb. 1983.

[25] H. Holma and A. Toskala, *WCDMA for UMTS - HSPA evolution and LTE*. John Wiely & Sons, 2010.

[26] A. Assalini, E. Dall'Anese, and S. Pupolin, "Linear MMSE MIMO channel estimation with imperfect channel covariance information," in *Proc. Intel. Cof. Communications (ICC)*, Jun. 2009.